"Smart" Self-Assembled Quantum Dots Regulate and Stabilize Structure in Phase-Separated Polymer Blends

Yunyong Guo and Matthew G. Moffitt*

Department of Chemistry, University of Victoria, P.O. Box 3065, Victoria, BC V8W 3V6, Canada

Received August 24, 2007. Revised Manuscript Received October 25, 2007

Cadmium sulfide (CdS) quantum dots (QDs) coated with mixed polystyrene (PS)/poly(methyl methacrylate) (PMMA) brush layers (PS/PMMA–CdS) self-assemble at the polymer/polymer interface of a phase-separating blend of the corresponding homopolymers, forming an encapsulating shell surrounding PMMA islands in a PS matrix. The segregated QDs regulate phase separation during spin-coating and dramatically stabilize the spin-coated blend morphologies during subsequent annealing, compared to neat PS:PMMA blends which undergo rapid phase inversion and coarsening. PS/PMMA–CdS QDs are shown to retain their photoluminescence following interfacial self-assembly and subsequent annealing. Free-standing arrays of polymer/QD rings formed via directed self-assembly can be developed by selective solvent washing and removal of homopolymers from the spin-coated films. This work demonstrates the principle that colloidal inorganic elements such as QDs, along with possessing interesting optical properties, can also play a key role in the self-organization and stability of polymer blend-based devices.

Introduction

Colloidal semiconductor quantum dots (QDs) and metal nanoparticles are widely recognized as potential functional elements in polymer-based devices due to their range of interesting optical and electronic properties. For many applications, engineering specific collective properties in polymer/nanoparticle composites will require controlled spatial organization of both organic and inorganic components on multiple length scales.[1–9] Several strategies for the dispersion and ordering of QDs and metal nanoparticles within polymers have been demonstrated, starting with hybrid building blocks consisting of an inorganic nanoparticle core and an external polymer brush stabilizing layer. Polymer-stabilized nanoparticles have been shown to undergo self-assembly in block copolymer films,[2–4] at the air–water interface,[5,6] in aqueous media,[1,7,8] and in phase-separating polymer blends,[9,10] leading to a wide range of hierarchical assemblies.

More recently, inorganic nanoparticles coated with mixed brushes of two different types of homopolymer chains have received considerable attention.[11–16] In response to various external stimuli, these "smart" particles undergo changes in surface properties via conformational rearrangements of the mixed polymer brush, introducing new possibilities for three-dimensional (3D) self-assembly into complex and controllable superstructures.[16] In our group, we have recently described the synthesis of cadmium sulfide (CdS) QDs with mixed polystyrene/poly(methyl methacrylate) (PS/PMMA) brush layers (designated PS/PMMA–CdS, Scheme 1), via micellization of a polystyrene-*b*-poly(acrylic acid)-*b*-poly(methyl methacrylate) (PS-*b*-PAA-*b*-PMMA) triblock copolymer, followed by growth of QDs in the PAA cores.[17] On the basis of static and dynamic light scattering results,

Scheme 1. Structure of PS/PMMA–CdS Mixed Brush-Stabilized QDs

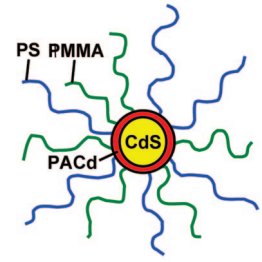

PS/PMMA-CdS

* To whom correspondence should be addressed.

(1) Shenhar, R.; Norsten, T. B.; Rotello, V. M. *Adv. Mater.* **2005**, *17*, 657.
(2) Bockstaller, M. R.; Mickiewicz, R. A.; Thomas, E. L. *Adv. Mater.* **2005**, *17*, 1331.
(3) Haryono, A.; Binder, W. H. *Small* **2006**, *2*, 600.
(4) Lin, Y.; Böker, A.; He, J.; Sill, K.; Xiang, H.; Abetz, C.; Li, X.; Wang, J.; Emrick, T.; Long, S.; Wang, Q.; Balazs, A.; Russell, T. P. *Nature (London)* **2005**, *434*, 55.
(5) Fahmi, A. W.; Oertel, U.; Steinert, V.; Froeck, C.; Stamm, M. *Macromol. Rapid Commun.* **2003**, *24*, 625.
(6) Cheyne, R. B.; Moffitt, M. G. *Macromolecules* **2007**, *40*, 2046.
(7) Kim, B.-S.; Qiu, J.-M.; Wang, J.-P.; Taton, T. A. *Nano Lett.* **2005**, *5*, 1987.
(8) Yusuf, H.; Kim, W.-G.; Lee, D.-H.; Aloshyna, M.; Brolo, A. G.; Moffitt, M. G. *Langmuir* **2007**, *23*, 5251.
(9) Wang, C.-W.; Moffitt, M. *Chem. Mater.* **2005**, *17*, 3871.
(10) Minelli, C.; Geissbuehler, I.; Eckert, R.; Vogel, H.; Heinzelmann, H.; Liley, M. *Colloid Polym. Sci.* **2004**, *282*, 1274.
(11) Li, D.; Sheng, X.; Zhao, B. *J. Am. Chem. Soc.* **2005**, *127*, 6248.
(12) Shan, J.; Nuopponen, M.; Jiang, H.; Viitala, T.; Kauppinen, E.; Kontturi, K.; Tenhu, H. *Macromolecules* **2005**, *38*, 2918.
(13) Shan, J.; Chen, J.; Nuopponen, M.; Viitala, T.; Jiang, H.; Peltonen, J.; Kauppinen, E.; Tenhu, H. *Langmuir* **2006**, *22*, 794.
(14) Chiu, J. J.; Kim, B. J.; Kramer, E. J.; Pine, D. J. *J. Am. Chem. Soc.* **2005**, *127*, 5036.
(15) Zubarev, E. R.; Xu, J.; Sayyad, A.; Gibson, J. D. *J. Am. Chem. Soc.* **2006**, *128*, 4958.
(16) Zubarev, E. R.; Xu, J.; Sayyad, A.; Gibson, J. D. *J. Am. Chem. Soc.* **2006**, *128*, 15098.
(17) Guo, Y.; Moffitt, M. G. *Macromolecules* **2007**, *40*, 5868.

10.1021/cm7024119 CCC: $37.00
Published on Web 11/30/2007

the stable mixed brush layers of the "smart" QDs were found to undergo changes in conformation in response to different solvent and polymer environments, allowing them to be dispersed in solvents of wide-ranging polarities and in films of either PS or PMMA homopolymers.

The mesoscale or microscale phase morphology of immiscible homopolymer blends plays a critical role in the performance of polymer-based photovoltaic and light-emitting devices[18] as well as being of generally interest for surface patterning applications.[9,19] Both types of applications can be severely limited by the thermodynamic tendency of blend films to undergo uncontrolled phase coarsening upon heating, driven by a combination of interfacial tension between polymer components and preferential interactions at the surface and substrate. Various studies demonstrate that phase morphologies can be regulated and stabilized by additives such as random copolymers,[20–24] block copolymers,[23,25] and inorganic nanoparticles,[26–29] generally known as compatibilizers, which tend to mitigate unfavorable interactions between immiscible blend components, usually by segregating at the polymer/polymer interface. To date, the role of added compatibilizers has been limited to lowering the interfacial tension or enhancing interfacial adhesion. However, as pointed out by Chung et al.,[28] the possibility of using absorbing and photoluminescent QDs as compatibilizers in polymer blend-based devices could lead to dual-functional nanoparticles which *both* stabilize the blend structure *and* impart specific optical properties to the final device.

In this paper, we show that CdS QDs coated with mixed polymer brushes (PS/PMMA–CdS) are driven to the polymer/polymer interface of phase-separating blends of PS and PMMA homopolymers during spin-coating, resulting in self-assembled photoluminescent rings of PS/PMMA–CdS encapsulating the dispersed PMMA phase. The directed organization of QDs arises from an overall lowering of interfacial tension between blend components due to the mixed polymer surface layer of PS/PMMA–CdS. Most importantly, we show that the interfacial segregation of mixed brush-stabilized QDs regulates the phase separation process during spin-coating and dramatically stabilizes the domain structure during subsequent annealing. This provides the first example of QDs acting as both compatibilizers and photoluminescent elements in a polymer blend, demonstrating the potential for expanding the role of QDs in polymer-based devices via appropriate design of the external polymer layer. This work also highlights unique opportunities for self-assembly of QDs into complex architectures within phase-separating polymer blend films via spontaneous interfacial segregation.

Experimental Section

Preparation of Spin-Coated Blend Films. Stock solutions of PS/PMMA–CdS, PS homopolymer, and PMMA homopolymer were prepared by codissolving appropriate quantities of each component in spectroscopic grade toluene to polymer concentrations of 6 wt %. The stock solutions were stirred for 4 h and left to stand overnight in the dark to equilibrate. Blend solutions of the desired composition were then prepared by filtering measured amounts of each stock solution through two membrane filters (0.45 μm nominal pore size) connected in series into glass sample vials. For all blends, the ratio of PS homopolymer to PMMA homopolymer was 30:70 (w:w), while the weight percentage of PS/PMMA–CdS QDs relative to the total polymer weight varied (0, 3, 10, 20, or 30%).

Before spin-coating, 18 × 18 mm glass microscope coverslips were cleaned by 30 min sonication in spectroscopic grade methanol, chloroform, and toluene, successively, and then dried overnight under vacuum at 70 °C. Various blend films were obtained by depositing one drop of blend solution on the glass substrate and spin-coating at 3000 rpm for 1 min. The blend films were then dried overnight under active vacuum at 25 ± 1 °C to remove any residual solvent. For annealing experiments, blend films were annealed in a vacuum oven at 150 ± 1 °C. After a designated time, annealed films were quenched in cold deionized water immediately after removal from the vacuum oven. To test reproducibility, several films were prepared for each blend composition and annealing period.

Some of the blend films were washed in selective solvents prior to atomic force microscopy (AFM) imaging in order to determine the lateral distribution of the various phases. To selectively remove the PS phase, films were placed in a Petri dish containing ~20 mL of cyclohexane and stirred for ~20 min, followed by washing several times with clean solvent. Using an identical procedure, acetic acid (99.7%) washing was used to selectively remove the PMMA phase. After allowing the washed films to air-dry under ambient conditions for 4 h, the films were dried overnight under active vacuum at 25 ± 1 °C overnight before AFM imaging.

Atomic Force Microscopy (AFM). A Veeco AFM Instrument equipped with a Veeco tip (Nanoprobe-MLCT-EXMT-A) running in contact mode was used to obtain AFM images. The effect of vibration was minimized by a vibration-resistant housing on a vibration isolation platform maintained at 80 psi. Each film was imaged several times at different locations on the substrate.

Laser Scanning Confocal Fluorescence Microscopy (LSCFM). Laser scanning confocal fluorescence microscopy measurements were carried out on a Zeiss LSM 410 equipped with an Ar/Kr laser. All films were excited at 488 nm, using a band-pass 485 ± 20 nm line selection filter and a FT 510 dichroic beam splitter. A long-pass 515 nm emission filter was employed such that only light above 515 nm reached the PMT. A Zeiss Plane-Aprochromat 63× oil-immersion objective was employed. A pinhole diameter of 1.31 Airy units was used for all measurements, resulting in an optical section thickness of 0.75 μm fwhm. Control films containing no PS/PMMA–CdS showed no significant detector signal under these conditions, confirming that light intensity in images of films containing PS/PMMA–CdS was due to QD emission.

(18) Moons, E. *J. Phys.: Condens. Matter* **2002**, *14*, 12235.
(19) Boltau, M.; Walheim, S.; Mlynek, J.; Krausch, G.; Steiner, U. *Nature (London)* **1998**, *391*, 877.
(20) Takenaka, M.; Hashimoto, T.; Dobashi, T. *Phys. Rev. E* **1995**, *52*, 5142.
(21) Lee, M. S.; Lodge, T. P.; Macosko, C. W. *J. Polym. Sci., Part B: Polym. Phys.* **1997**, *35*, 2835.
(22) Russo, A. P.; Nauman, E. B. *J. Polym. Sci., Part B: Polym. Phys.* **2000**, *38*, 1301.
(23) Barham, B.; Fosser, K.; Voge, G.; Waldow, D.; Halasa, A. *Macromolecules* **2001**, *34*, 514.
(24) Winey, K. I.; Berba, M. L.; Galvin, M. E. *Macromolecules* **1996**, *29*, 2868.
(25) Adedeji, A.; Lyu, S.; Macosko, C. W. *Macromolecules* **2001**, *34*, 8663.
(26) Tanaka, H.; Lovinger, A. J.; Davis, D. D. *Phys. Rev. Lett.* **1994**, *72*, 2581.
(27) Ginzburg, V. V.; Qiu, F.; Paniconi, M.; Peng, G.; Jasnow, D.; Balazs, A. C. *Phys. Rev. Lett.* **1999**, *82*, 4026.
(28) Chung, H.-J.; Ohno, K.; Fukuda, T.; Composto, R. J. *Nano Lett.* **2005**, *5*, 1878.
(29) Minelli, C.; Frommen, C.; Hinderling, C.; Pugin, R.; Heinzelmann, H.; Liley, M. *Colloid Polym. Sci.* **2006**, *284*, 482.

Transmission Electron Microscopy (TEM). TEM was performed on a Hitachi H-700 electron microscope, operating on an accelerating voltage of 75 keV. Blend films were embedded in an Epon resin, and then ~50 nm thick sections were obtained with a diamond knife on Reichert UltraCut E ultramicotome. The thin sections were then placed on carbon/Formvar-coated 300 mesh copper grids for imaging.

Photoluminescence Measurements. Static photoluminescence (PL) measurements were recorded on an Edinburgh Instruments FLS 920 instrument equipped with a Xe 450 W arc lamp and a red-sensitive PMT (R928-P). All spectra were obtained using an excitation wavelength of 400 nm and a 420 nm bandpass filter and recorded at 1 nm spectral resolution. For the PL measurements of blend films, back-face excitation with an incidence angle of 30° to the substrate normal was employed.

Analysis of AFM Surface Features. To determine the mean heights and diameters of surface features after various selective solvent treatments, at least four different regions of each film were imaged. Feature topologies were measured using the AFM software (SPM laboratory), with more than 100 individual domains measured for each sample.

To determine surface correlation lengths, Λ_m, radial average plots of fast Fourier transform (FFT) power spectra from AFM images were obtained; for each FFT spectrum, 25 different line profiles were averaged to produce plots of intensity $I(q)$ vs scattering vector q. The dominant wave vector q_m was determined from a Gaussian fit to the main scattering peak, from which the correlation length was calculated using $\Lambda_m = 2\pi/q_m$.

Results and Discussion

The synthesis and characterization of cadmium sulfide (CdS) QDs with mixed polystyrene/poly(methyl methacrylate) (PS/PMMA) stabilizing layers, designated PS/PMMA–CdS (Scheme 1), have been recently described in our previous publication.[17] From the UV–vis absorption threshold, $\lambda_{thresh} = 512$ nm, a QD diameter of ~7 nm is determined, corresponding to the high end of the QD size distribution. From static light scattering analysis, an average CdS QD is surrounded by a collapsed layer of ~200 poly(cadmium acrylate) (PACd) chains, which is covalently attached to an external brush layer consisting of an equal number of randomly distributed PS and PMMA chains (~200 chains of each type), with molecular weights M_n = 30 800 and 23 600 g/mol, respectively; from the measured aggregation number and estimated core size (QD + PACd), the surface density of the mixed brush is ~0.8 chains/nm^2.[17] The overall hydrodynamic diameter of PS/PMMA–CdS QDs in toluene was determined by dynamic light scattering (DLS) to be 62 nm.

Blend solutions of PS and PMMA homopolymers of composition PS:PMMA = 30:70 (w/w) were obtained by mixing stock solutions of each component in toluene. PS homopolymer (M_n = 130 000 g/mol, M_w/M_n = 1.01) was prepared in our laboratory by anionic polymerization, and PMMA homopolymer (M_w = 120 000 g/mol) was purchased from Aldrich. Various quantities of PS/PMMA–CdS QDs dispersed in toluene were added to obtain a series of blend solutions with a constant PS:PMMA ratio (30:70) and various PS/PMMA–CdS contents: 0, 10, 20, and 30% (w/w), relative to the total polymer mass. Blend films were then obtained by spin-coating each solution onto clean glass substrates at 3000 rpm. Blend film thicknesses determined from AFM scratch tests were between 120 and 200 nm.

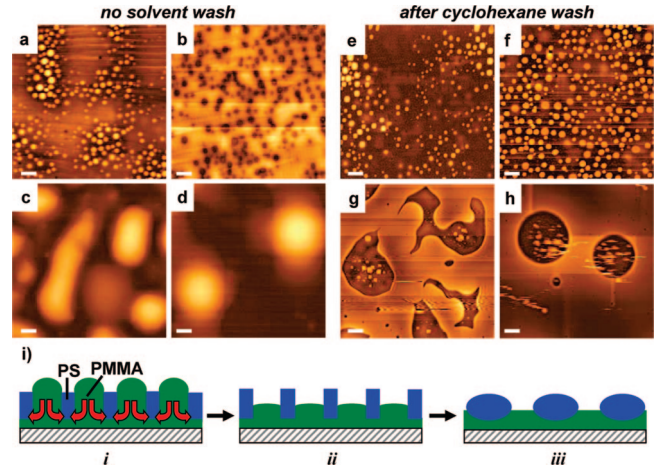

Figure 1. Atomic force microscopy (AFM) images of neat PS:PMMA (30:70) blend films for various periods of annealing at 150 °C following spin-coating. In (a–d), films were imaged with no selective solvent washing; in (e–h), films were washed with cyclohexane to remove the PS phase. (a, e) 0 h annealing; (b, f) 4 h annealing; (c, g) 8 h annealing; (d, h) 24 h annealing. All scale bars represent 2 μm. (i) shows a schematic (not to scale) of the PS and PMMA phase distributions following spin-coating (*i*) and for different stages of phase coarsening (*ii*, *iii*), as described in the text.

The morphologies of thin PS:PMMA blend films after spin-coating and with subsequent annealing have been widely investigated;[30–35] results for our control films without added PS/PMMA–CdS are consistent with previous studies. Figure 1 shows atomic force microscopy images (AFM, Veeco Instruments) of PS:PMMA films immediately after spin-coating (a, e) and following 4 h (b, f), 8 h (c, g) and 24 h (d, h) annealing at 150 °C. In Figure 1e–h, the films were washed with cyclohexane prior to AFM imaging, selectively dissolving the PS phase and allowing PS and PMMA domains to be identified. Comparing parts a and e of Figure 1, it is apparent that the spin-coated blend morphology (no annealing) consists of small PMMA islands protruding above a continuous layer of PS. Selectively dissolving the PMMA phase with acetic acid was found to remove the entire film, including the PS phase, from the glass (not shown); this indicates that the PMMA islands are attached to a continuous PMMA wetting layer at the substrate (Figure 1i, *i*), as previously reported.[31,33,35]

The morphology of spin-coated PS:PMMA blends is the result of a surface-oriented phase separation process, which becomes trapped in a nonequilibrium state by fast solvent evaporation. Annealing the neat PS:PMMA films thus resulted in dramatic changes in the film structure, as the system evolved in the direction of a more favorable free energy state. First, the island morphology rapidly transformed into a pitted structure (Figure 1b,f) as the protruding PMMA domains drained into the continuous PMMA bottom layer

(30) Tanaka, K.; Takahara, A.; Kajiyama, T. *Macromolecules* **1996**, *29*, 3232.
(31) Walheim, S.; Boltau, M.; Mlynek, J.; Krausch, G.; Steiner, U. *Macromolecules* **1997**, *30*, 4995.
(32) Harris, M.; Appel, G.; Ade, H. *Macromolecules* **2003**, *36*, 3307.
(33) Zong, Q.; Li, Z.; Xie, X. *Macromol. Chem. Phys.* **2004**, *205*, 1116.
(34) Heriot, S. Y.; Jones, R. A. L. *Nat. Mater.* **2005**, *4*, 782.
(35) Li, Y.; Yang, Y.; Yu, F.; Dong, L. *J. Polym. Sci., Part B: Polym. Phys.* **2006**, *44*, 9.

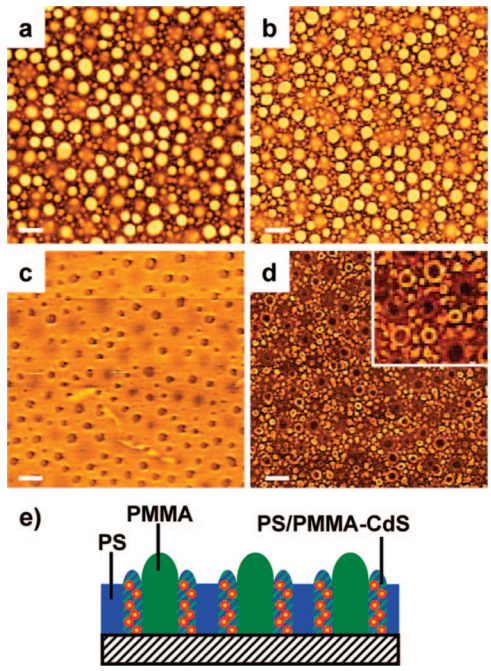

Figure 2. Atomic force microscopy (AFM) images of PS:PMMA (30:70) blend films with 10% PS/PMMA–CdS QDs following spin-coating: (a) film without solvent washing; (b) film washed with cyclohexane to remove the PS phase only; (c) film washed with acetic acid to remove the PMMA phase only; (d) film washed with cyclohexane then acetic acid to remove both the PS and PMMA phases; the remaining rings of PS/PMMA–CdS indicate interfacial self-assembly of QDs during spin-coating. All scale bars represent 2 μm; the dimensions of inset to (d) are 5 μm × 5 μm. (e) shows a schematic (not to scale) of phase distributions in the spin-coated film with relative heights of the PS, PMMA, and PS/PMMA–CdS phases.

(Figure 1i, *ii*). Next, rupture of the PS top layer occurred due to unfavorable interactions between PS and PMMA (Figure 1c,g). Subsequent phase coarsening resulted in tall (~500 nm) circular PS droplets (Figure 1d,h) resting on top of a bottom layer of PMMA (Figure 1i, *iii*).

Figure 2a–d shows AFM data of spin-coated PS:PMMA (30:70) blends containing 10% PS/PMMA–CdS QDs.[36] The series of images represents different selective solvent treatments following spin-coating, from which the lateral distribution of the various phases were determined. Comparison of Figure 2a (no solvent wash), Figure 2b (cyclohexane wash, PS removal), and Figure 2c (acetic acid wash, PMMA removal) indicates a morphology consisting of PMMA islands within a PS matrix, similar to the neat PS:PMMA blend. Removal of both PS and PMMA phases (cyclohexane and then acetic acid wash) shows the location of the PS/PMMA–CdS QDs within the ternary blend (Figure 2d): a clear distribution of free-standing rings reveals that the PS/PMMA–CdS QDs self-assembled at the PS/PMMA interface during spin-coating, forming an encapsulating phase surrounding the PMMA islands.

From topographic analysis of the AFM images in Figure 2 (not shown), the heights of the three phases relative to glass were determined. AFM film topologies before and after washing with cyclohexane show the average height of the PS matrix to be ~70 nm compared to ~130 nm for the PMMA islands. After removal of both PS and PMMA homopolymers, the remaining PS/PMMA–CdS rings have an intermediate height of ~85 nm. These relative heights are explained by the effect of different affinities of the three components for the solvent during spin-coating, with PS having the highest affinity for toluene and PMMA having the lowest.[31] Following phase separation, the PS-rich phase will contain the most solvent and will therefore collapse to a level below that of the other two phases when the last of the toluene evaporates; this leaves a topology of relatively tall PMMA islands surrounded by PS/PMMA–CdS rings of intermediate height. We note that solvent swelling of the PS phase, and the relative increase in its volume fraction during spin-coating, also explains why PS constitutes the matrix phase in the spin-coated films, despite PMMA being the major polymer component.

Another marked effect of adding 10% PS/PMMA–CdS QDs to the spin-coated blends is the absence of a PMMA wetting layer at the glass substrate, in contrast to the phase distribution in the neat blend. This is most evident from AFM data after selective solvent treatment: washing the blend film with acetic acid (Figure 2c) was found to remove the PMMA domains while leaving the PS matrix intact, indicating that PS does not rest on top of a bottom layer of PMMA. A possible explanation is that, in the early stages of spin-coating when sufficient toluene is still present, PS/PMMA–CdS QDs may partition between the PS-rich and PMMA-rich phases. As a result, the nonpolar styrene segments from PS/PMMA–CdS would lower the affinity of the PMMA phase for the polar glass substrate. Figure 2e summarizes the blend morphology determined from AFM data in Figure 2a–d, with PS, PMMA, and PS/PMMA–CdS regions each spanning the entire film.

The localization of PS/PMMA–CdS QDs at the PS/PMMA interface during spin-coating is a function of their mixed polymer brush surface layer, which governs nanoparticle interactions with the surrounding environment. QD segregation is observed to be complete on the time scale of spin-coating, in contrast to the study of Chung et al. in which interfacial self-assembly of surface-modified silica nanoparticles occurred during subsequent annealing.[28] To a simple approximation, the exterior of PS/PMMA–CdS QDs resembles a poly(styrene-*co*-methyl methacrylate) random copolymer, consisting of an isotropic distribution of styrene and methyl methacrylate segments. The location of a polymer 3 in a phase-separated mixture of polymer 1 (dispersed phase) and polymer 2 (matrix phase) has been described by Hobbs et al.[37] using spreading coefficients λ_{31}, and λ_{13}, defined as

$$\gamma_{31} = \gamma_{12} - [\gamma_{31} + \gamma_{23}]; \quad \gamma_{13} = \gamma_{23} - [\gamma_{31} + \gamma_{12}] \qquad (1)$$

where γ_{ij} are interfacial tensions between components i and j. If $\lambda_{31} > 0$ and $\lambda_{13} < 0$, then polymer 3 will form a shell encapsulating polymer 1, whereas polymer 3 will tend to form a separate dispersed phase if λ_{31} and λ_{13} are both negative. When polymer 3 is a random copolymer made up of repeat units of polymers 1 and 2, Lee et al. have used a binary interaction model to show that encapsulation of the dispersed phase is strongly favored,[21] in agreement with

(36) The CdS content of PS/PMMA–CdS is ~5 wt %, so that the inorganic content of these blends is in fact extremely low.

(37) Hobbs, S. Y.; Dekkers, M. E. J.; Watkins, V. H. *Polymer* **1988**, *29*, 1598.

experimental evidence.[21,24] The mixed polymer surface layer of PS/PMMA–CdS QDs thus directs their self-assembly at the PS/PMMA interface, driven by an overall decrease in the interfacial tension of blend components.

We note that this simplified picture, based on binary enthalpic interactions between pairs of PS and PMMA segments, does not include possible entropic "dry brush" effects, which can also play an important role in determining the segregation of polymer brush-coated nanoparticles in block copolymers and homopolymer matrices.[38] In our previous work on QDs coated with *homogeneous* PS brush layers with molecular weight and surface density similar to the mixed brush particles considered here,[39] we found that the QDs localized within the PS phase of PS/PMMA polymer blends during solvent evaporation, rather than segregating to the polymer/polymer interface; as well, in PS homopolymers of various molecular weights, the PS-coated QDs remained well dispersed even after 8 days of annealing, with no evidence of autophobic phase separation, except at extremely high nanoparticle loadings (50 wt %).[39] This suggests that the interfacial segregation observed in the present system is primarily due to the mixture of segments in the brush layer rather than to "dry brush" effects. However, entropic effects should be further considered in future work by investigating the influence of the mixed brush density and the molecular weights of brush and homopolymer chains on interfacial segregation.

Annealing the spin-coated blend films for various times at 150 °C reveals a dramatic stabilizing effect of 10% PS/PMMA–CdS QDs on the polymer blend morphology (Figure 3a–d). Compared to the surface topology immediately after spin-coating (Figure 2a), the distribution and size of the PMMA islands remain constant during annealing. This is in marked contrast to the rapid phase inversion and domain coarsening observed for the neat PS:PMMA blend films (Figure 1). Washing the annealed films with cyclohexane and acetic acid shows that the PS/PMMA–CdS QDs remain localized at the PS/PMMA interface throughout the annealing process (Figure 3d, inset).

The phase coarsening of blend films with different PS/PMMA–CdS QD contents was quantified via fast Fourier transforms (FFT) of AFM surface morphologies. From the dominant wave vectors, q_m, of FFT-AFM power spectra, the correlation lengths of the surface morphologies, defined as $\Lambda_m = 2\pi/q_m$, were determined for various annealing times (Figure 3e). For the control PS:PMMA blend (0% PS/PMMA–CdS), the plot of Λ_m vs t shows a large increase in Λ_m over the 48 h annealing period, with three distinct growth regions associated with the various stages of surface morphology evolution observed in Figure 1. By comparison, when 3% PS/PMMA–CdS is added to the blend, the coarsening process is slowed significantly, with a relatively small increase in Λ_m over 48 h. Moreover, for the 10% and 20% PS/PMMA–CdS blends, the spin-coated morphologies

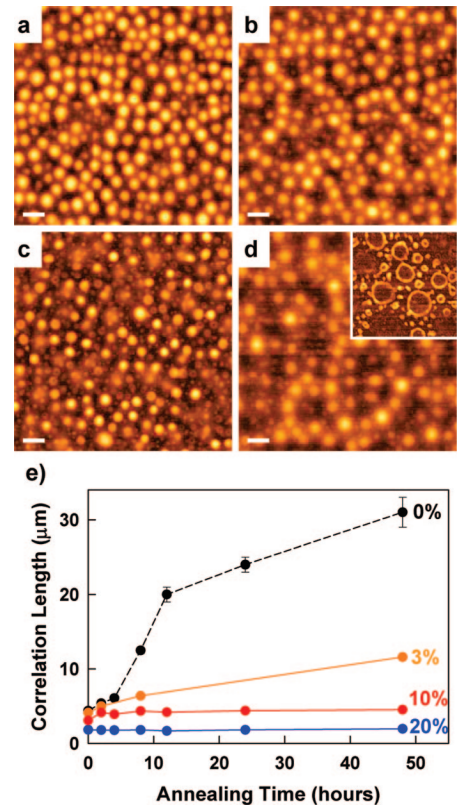

Figure 3. Atomic force microscopy (AFM) images of PS:PMMA (30:70) blend films with 10% added PS/PMMA–CdS QDs for various periods of annealing at 150 °C following spin-coating: (a) 4 h annealing; (b) 8 h annealing; (c) 12 h annealing; (d) 24 h annealing. Inset to (d) shows film washed with cyclohexane and then acetic acid to reveal the distribution of PS/PMMA–CdS QDs. All scale bars represent 2 μm; the dimensions of inset to (d) are 5 μm × 5 μm. (e) Plots of the surface correlation length, Λ_m, vs annealing time for different PS/PMMA–CdS QD contents. Λ_m is determined from fast Fourier transforms (FFT) of AFM images, as described in the text.

are found to be pinned by the added QDs, with Λ_m values for these films remaining constant throughout the annealing process (with the exception of a very small initial increase in the 10% PS/PMMA–CdS film). This stabilizing effect is consistent with a decrease in interfacial tension caused by the localization of PS/PMMA–CdS QDs during spin-coating, which lowers the driving force for phase coarsening during annealing. In addition, the absence of a PMMA wetting layer in the QD-containing blends should provide kinetic stabilization relative to the neat blends, in which the first stage of phase coarsening is the fast hydrodynamic flow of PMMA islands into the connected PMMA bottom layer (Figure 1).

Along with imparting thermal stability during annealing, the interfacial segregation of PS/PMMA–CdS QDs also regulates the domain morphology during spin-coating. The effect of different PS/PMMA–CdS QD contents on blend morphologies immediately following spin-coating is illustrated by transmission electron microscopy (TEM, Hitachi H-700) of microtomed sections cut parallel to the plane of the films (Figure 4). For the neat blend (0% PS/PMMA–CdS, Figure 4a), the internal film morphology consists of small PMMA domains (white), with mean diameter ~400 nm, in a matrix of PS (dark gray). With the addition of 10% PS/

(38) (a) Bansal, A.; Yang, H.; Li, C.; Cho, K.; Benicewicz, B. C.; Kumar, S. T.; Schadler, L. S. *Nat. Mater.* **2005**, *4*, 693. (b) Corbierre, M. K.; Cameron, N. S.; Sutton, M.; Laaziri, K.; Lennox, R. B. *Langmuir* **2005**, *21*, 6063. (c) Chiu, J. J.; Kim, B. J.; Yi, G.-R.; Bang, J.; Kramer, E. J.; Pine, D. J *Macromolecules* **2007**, *40*, 3361.

(39) Wang, C.-W.; Moffitt, M. G. *Langmuir* **2005**, *21*, 2465.

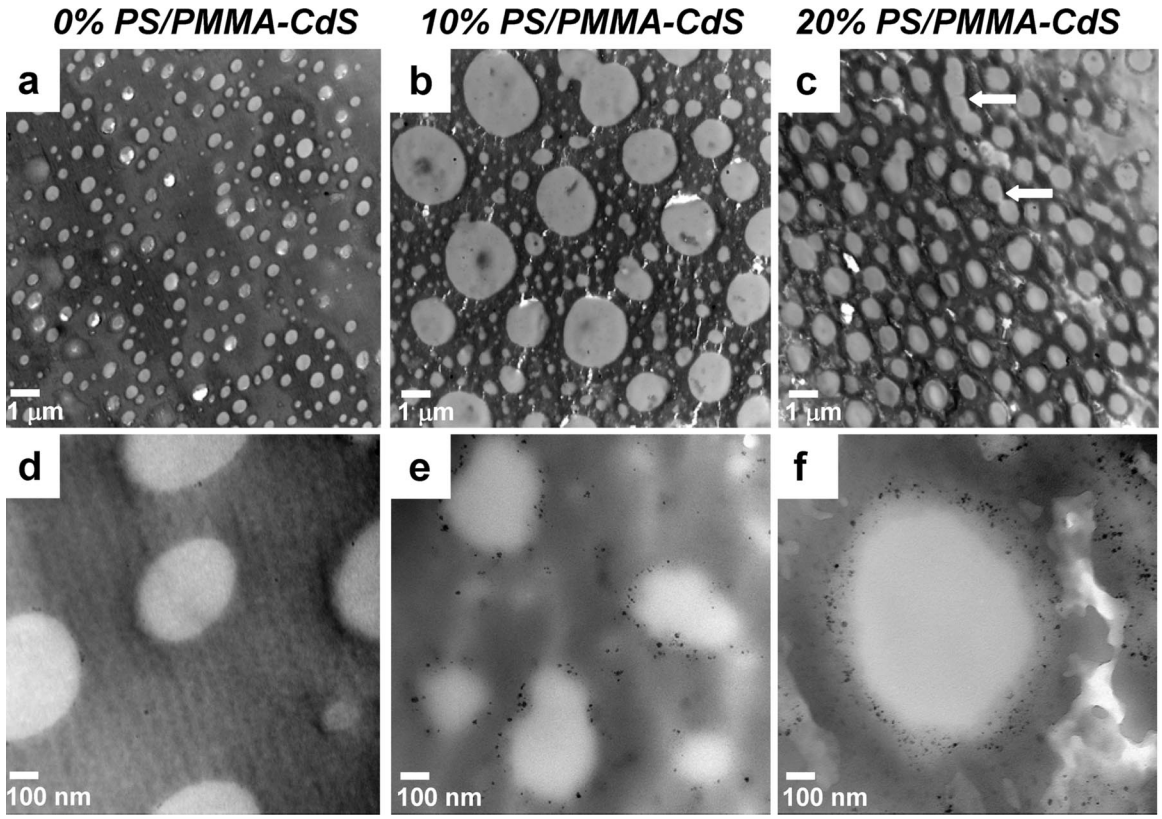

Figure 4. Transmission electron microscopy (TEM) images of parallel sections of PS:PMMA (30:70) blend films with (a, d) 0%, (b, e) 10%, and (c, f) 20% added PS/PMMA–CdS QDs.

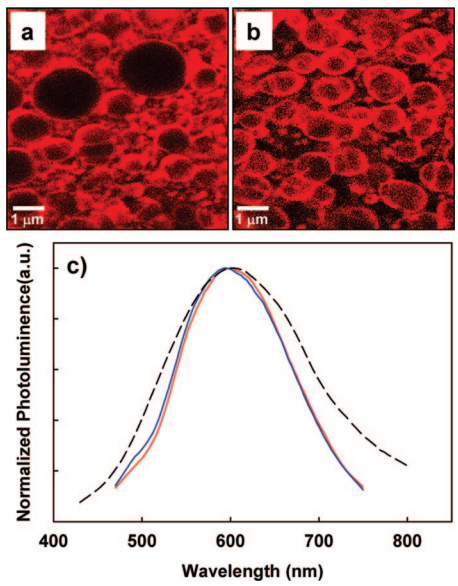

Figure 5. Laser scanning confocal fluorescence microscopy (LSCFM) images of PS:PMMA (30:70) blend films with (a) 10% and (b) 20% added PS/PMMA–CdS QDs. (c) Normalized photoluminescence (PL) spectra of blend films in (a) (red line) and (b) (blue line); PL spectrum of PS/PMMA–CdS QDs dispersed in toluene (dashed line) is shown for comparison.

PMMA–CdS QDs (Figure 4b), the PMMA domain size actually increases relative to the control blend, despite a lowering of interfacial tension. This can be understood in terms of PS/PMMA–CdS QDs preventing accumulation of PMMA at the substrate, as discussed above, which will increase the amount of PMMA in the PS matrix, and thus the domain size, relative to the neat blend. Size distribution analysis reveals a clearly bimodal distribution of PMMA domains in the 10% PS/PMMA–CdS blend (Supporting Information), with mean sizes of ∼400 and ∼1600 nm for the two separate domain populations.[40] The regulating effect of PS/PMMA–CdS QDs on phase separation is evident by comparison of the 10% and 20% PS/PMMA–CdS blends (Figure 4b,c). With increased PS/PMMA–CdS QD content, the PMMA domains show a mean diameter of ∼700 nm and are significantly less polydispersed than the 10% PS/PMMA–CdS blend; notably, the population of large domains (>1000 nm) is no longer present, indicating that domain coalescence is suppressed. We also observe several linear PMMA regions in the 20% PS/PMMA–CdS blend (Figure 4c, white arrows) which appear to be trapped in the process of pinching into circular domains, suggesting the remnants of a percolation-to-cluster transition from a bicontinuous phase structure. The difference between the film morphologies in the 10% and 20% PS/PMMA–CdS blends can be explained by either a decrease in the rate of domain coarsening or a shift in the thermodynamic boundary for phase separation, such that earlier domain structures are trapped by solvent evaporation as the PS/PMMA–CdS content is increased. From these results, therefore, it appears that the addition of mixed brush-coated QDs to polymer

(40) We note that the larger PMMA domains in the 10% PS/PMMA–CdS blend do not protrude significantly above the PS phase and so are not detected in the AFM images in Figures 3 and 4. TEM of film sections of the 10% and 20% PS/PMMA–CdS blends after 24 h annealing (Supporting Information) confirms that the internal film morphologies, along with the surface features tracked by AFM, are stable to annealing.

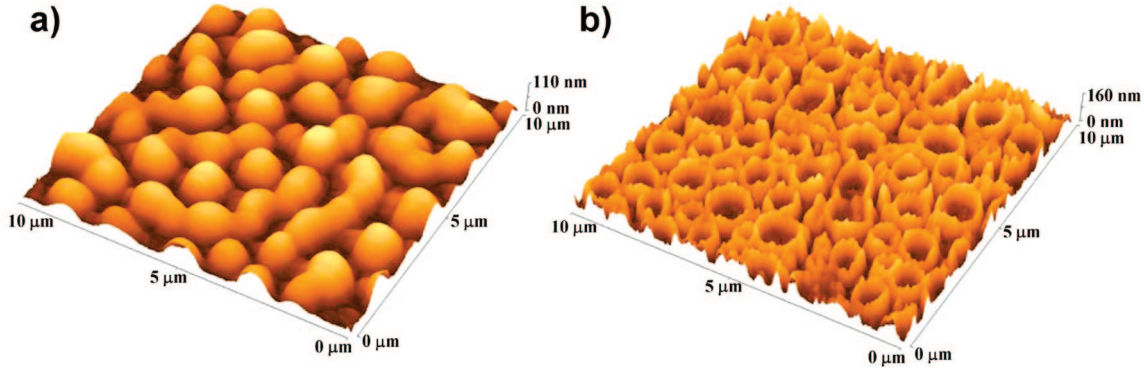

Figure 6. Three-dimensional (3D) atomic force microscopy (AFM) images of PS:PMMA (30:70) blend films with 20% added PS/PMMA–CdS QDs: (a) film obtained by spin-coating and 8 h annealing at 150 °C, with no solvent washing; (b) film obtained by spin-coating and 8 h annealing at 150 °C, followed by solvent washing with cyclohexane and then acetic acid to remove the PS and PMMA phases, respectively. Nearly identical blend morphologies were obtained by spin-coating and solvent development without annealing.

blend films should provide routes to a range of thermally stable domain structures of technological interest, including mesoscale bicontinuous morphologies for polymeric OLED and photovoltaic devices.

Higher magnification TEM of the PS/PMMA interface in the control blend (0% PS/PMMA–CdS) is shown in Figure 4d. TEM images of the 10% and 20% PS/PMMA–CdS blends at the same magnification (parts e and f of Figure 4, respectively) confirm that the QDs (black dots) are localized at the interface between the PMMA domains (white) and the PS matrix (dark gray). The QDs are seen to be dispersed within an encapsulating shell of mixed PS and PMMA chains (light gray) surrounding the PMMA islands, supporting the AFM data discussed previously. From comparison of parts e and f of Figure 4, it is noted that the thickness of the encapsulating phase increases when the PS/PMMA–CdS content increases from 10% to 20%.

In addition to the compatibilizing effect afforded by their mixed polymer brush layers, PS/PMMA–CdS nanoparticles exhibit the interesting photoluminescence (PL) associated with their QD cores. Laser scanning confocal fluorescence microscopy (LSCFM, Zeiss LSM-410) of the 10% and 20% PS/PMMA–CdS blend films shows PL rings from localized QDs surrounding PMMA domains within the phase-separated films (Figure 5a,b); the PL from assembled QDs following spin-coating was found to persist with long periods of annealing (Supporting Information). PL spectra of the blend films are very similar to that of the individual PS/PMMA–CdS particles dispersed in dilute toluene solution (Figure 5c), indicating that the QD optical properties are retained during phase separation and interfacial self-assembly. The slight narrowing of the ~600 nm trap state emission peak relative to QD PL in toluene is attributed to scattering effects within the blend film.

The interfacial organization of stable QDs with interesting optical function opens up intriguing possibilities for tuning and enhancing the collective properties of polymer blend-based device structures.[28] In addition, we note that this system provides a general route to novel patterned surfaces, including mesoscale arrays of polymer/QD rings. These hierarchical structures form as a result of interfacial self-assembly in the fast spin-coating process and can be subsequently "developed" by removal of the two homopolymer phases using selective solvents (Figure 6).

Conclusions

We have shown that CdS QDs with external mixed polymer brush layers of PS and PMMA chains are driven to the interface of PS:PMMA blends during spin-coating, regulating the domain size and stabilizing the phase-separated blend morphologies during subsequent annealing. This work underlines the principle that colloidal inorganic elements such as QDs, which are widely recognized for their interesting optical properties, can also play an important role in the self-organization and stability of polymer blend-based devices. As the present example shows, such systems can take advantage of appropriate polymer surface layers to control the interactions between nanoparticle and homopolymer components, providing new opportunities for tunable collective function via synergistic self-assembly.

Acknowledgment. The authors gratefully acknowledge the Natural Science and Engineering Research Council of Canada (NSERC), the Canadian Foundation for Innovation (CFI) and the British Columbia Knowledge Development Fund (BCKDF) for their support of the research.

Supporting Information Available: Size distributions of PMMA domain sizes for different PS/PMMA–CdS contents; TEM of 10% and 20% PS/PMMA–CdS blends after 24 h annealing; TEM of 30% PS/PMMA–CdS blend after 24 h annealing; LSCFM of 10% PS/PMMA–CdS blend after 24 h annealing. This material is available free of charge via the Internet at http://pubs.acs.org.

CM7024119